Am J Physiol Heart Circ Physiol 294: H2736–H2742, 2008.
First published April 18, 2008; doi:10.1152/ajpheart.00796.2007.

Effective arterial elastance as an index of pulmonary vascular load

Philippe Morimont,[1] Bernard Lambermont,[1] Alexandre Ghuysen,[1] Paul Gerard,[2] Philippe Kolh,[1] Patrizio Lancellotti,[3] Vincent Tchana-Sato,[1] Thomas Desaive,[1] and Vincent D'Orio[1]

[1]*Hemodynamics Research Laboratory (HemoLiege), University Hospital of Liege,* [2]*Statistics Institute, University of Liege, and* [3]*Cardiology Department, University Hospital of Liege, Liege, Belgium*

Submitted 10 July 2007; accepted in final form 16 April 2008

Morimont P, Lambermont B, Ghuysen A, Gerard P, Kolh P, Lancellotti P, Tchana-Sato V, Desaive T, D'Orio V. Effective arterial elastance as an index of pulmonary vascular load. *Am J Physiol Heart Circ Physiol* 294: H2736–H2742, 2008. First published April 18, 2008; doi:10.1152/ajpheart.00796.2007.—The aim of this study was to test whether the simple ratio of right ventricular (RV) end-systolic pressure (Pes) to stroke volume (SV), known as the effective arterial elastance (E_a), provides a valid assessment of pulmonary arterial load in case of pulmonary embolism- or endotoxin-induced pulmonary hypertension. Ventricular pressure-volume (PV) data (obtained with conductance catheters) and invasive pulmonary arterial pressure and flow waveforms were simultaneously recorded in two groups of six pure Pietran pigs, submitted either to pulmonary embolism (*group A*) or endotoxic shock (*group B*). Measurements were obtained at baseline and each 30 min after injection of autologous blood clots (0.3 g/kg) in the superior vena cava in *group A* and after endotoxin infusion in *group B*. Two methods of calculation of pulmonary arterial load were compared. On one hand, E_a provided by using three-element windkessel model (WK) of the pulmonary arterial system [E_a(WK)] was referred to as standard computation. On the other hand, similar to the systemic circulation, E_a was assessed as the ratio of RV Pes to SV [E_a(PV) = Pes/SV]. In both groups, although the correlation between E_a(PV) and E_a(WK) was excellent over a broad range of altered conditions, E_a(PV) systematically overestimated E_a(WK). This offset disappeared when left atrial pressure (Pla) was incorporated into E_a [$E_a * (PV) = (Pes - Pla)/SV$]. Thus $E_a * (PV)$, defined as the ratio of RV Pes minus Pla to SV, provides a convenient, useful, and simple method to assess the pulmonary arterial load and its impact on the RV function.

hemodynamics; pulmonary hypertension; right ventricle; ventriculo-arterial coupling

IN CURRENT CLINICAL practice, pulmonary arterial load [or right ventricular (RV) afterload] is usually expressed as the mean pulmonary vascular resistance, computed as the ratio of the pressure drop through the pulmonary circulation [difference between mean pulmonary arterial pressure (PAP_{mean}) and left atrial pressure (Pla)] to the mean pulmonary blood flow [cardiac output (CO)]. Such an evaluation ignores the pulsatile nature of both pressure and flow. Although oscillatory components of the pulmonary arterial load are low, and mean resistance may be a valuable index of the pulmonary vascular load, the pulsatile nature of the load may be prominent in numerous pathological situations. Wave reflections play an important role and should be taken into account in pulmonary hypertension resulting from several pathological conditions, like pulmonary embolism and septic shock (1, 2, 5, 14). In this way, the pulmonary arterial impedance spectrum, which is defined in the frequency domain, provides a more precise and complete description of the pulmonary vascular load (12, 17). However, because of its complexity, this approach is difficult to use in clinical practice and to link with data obtained in the time domain. Sunagawa et al. introduced the concept of the effective arterial elastance (E_a), defined as a steady-state arterial parameter that incorporates the principal elements of the windkessel model of the pulmonary vascular bed (24, 25). According to this concept, E_a is computed by combining the pulmonary vascular compliance, the characteristic impedance, and the resistance of the main pulmonary vessels, as well as the pulmonary peripheral resistance. An alternative method consists in assessing E_a by the steady-state ratio of end-systolic pressure to stroke volume (Pes/SV). This ratio can be simply obtained from steady-state ventricular pressure-volume (PV) measurements, while the pulmonary impedance spectrum or the windkessel parameters require simultaneous pulmonary arterial flow and pressure waveform acquisition. Moreover, the ratio of end-systolic ventricular elastance to E_a, obtained from PV relations, characterizes the ventriculo-arterial interaction. In the systemic circulation, both normal and hypertensive human subjects show good agreement between E_a computed using left ventricular PV loop and E_a calculated from windkessel model parameter value recorded in the aorta (10). In the pulmonary circulation, it remains unknown whether or not E_a(PV) can be used as a substitute of E_a(WK) [WK denotes E_a derivation from windkessel model]. Therefore, the purpose of the present study was to assess the validity of E_a(PV) derived from steady-state RV PV data in experimental animals insulted with endotoxin or submitted to clot embolism.

METHODS

All experimental procedures and protocols used in this investigation were reviewed and approved by the ethical committee of the Medical Faculty of the University of Liege and conformed to the *Guide for the Care and Use of Laboratory Animals* published by the US National Institutes of Health (NIH publication no. 85-23, revised 1996). Experiments were performed on two groups of six healthy pure Pietran pigs of either sex, weighing from 16 to 28 kg. The animals were premedicated with intramuscular administration of ketamine (20 mg/kg) and diazepam (1 mg/kg). Anesthesia was then induced and maintained by a continuous infusion of sufentanil (0.5 $\mu g \cdot kg^{-1} \cdot h^{-1}$) and pentobarbital (5 $mg \cdot kg^{-1} \cdot h^{-1}$). Spontaneous movements were prevented by pancuronium bromide (0.2 $mg \cdot kg^{-1} \cdot h^{-1}$). After endotracheal intubation via a cervical tracheostomy, the pigs were connected to a volume-cycled ventilator (Evita 2, Drager, Lubeck, Germany) set to deliver a tidal volume of 10 ml/kg at a respiratory rate of 20 breaths/min with an inspired O_2 fraction of 0.4. End-tidal CO_2

Address for reprint requests and other correspondence: P. Morimont, Medical Intensive Care Unit, Univ. Hospital of Liege, 4000 Liege, Belgium (e-mail: ph.morimont@chu.ulg.ac.be).

The costs of publication of this article were defrayed in part by the payment of page charges. The article must therefore be hereby marked "*advertisement*" in accordance with 18 U.S.C. Section 1734 solely to indicate this fact.

measurements (Capnomac, Datex, Helsinki, Finland) were used to monitor the adequacy of ventilation. Respiratory settings were adjusted to maintain end-tidal CO_2 between 30 and 35 Torr. The pulmonary trunk was exposed via a median sternotomy. A micromanometer-tipped catheter (Sentron pressure measuring catheter, Cordis, Miami, FL) was inserted into the main pulmonary artery through a stab wound in the RV outflow tract. A 14-mm-diameter perivascular flow-probe (Transonic Systems, Ithaca, NY) was placed around the main pulmonary artery 2 cm downstream from the pulmonary valve. The micromanometer-tipped catheter was manipulated so that the pressure sensor was finally positioned at the level of the flow probe. Pla was measured with a micromanometer-tipped catheter inserted into the cavity through the left atrial appendage. Systemic arterial blood pressure was monitored via a micromanometer-tipped catheter inserted into the abdominal aorta through the left femoral artery. A 7-F, 12-electrode (8-mm interelectrode distance) conductance micromanometer-tipped catheter (CD Leycom, Zoetermeer, the Netherlands) was inserted through the RV infundibulum into the RV and positioned so that all electrodes were in the RV cavity. A 6-F Fogarty balloon catheter (Baxter Healthcare, Oakland, CA) was advanced into the inferior vena cava through a right femoral venotomy. Inflation of this balloon produced a gradual preload reduction.

Experimental protocol. After surgical preparation, the animals were allowed to stabilize for 30 min. Baseline hemodynamic recording was performed, including PAP_{mean}, pulmonary blood flow ($\dot{Q}$), Pla, mean arterial blood pressure, and heart rate (HR). In the first group (*group A*), autologous blood clots (0.3 g/kg) were injected in the superior vena cava immediately after baseline measurements. In the second group (*group B*), the animals had an intravenous infusion of 0.5 mg/kg of a freshly prepared endotoxin solution (lipopolysaccharide from *E. coli* serotype 0127:B8, Sigma, St. Louis, MO) over 30 min at *time 0*.

Data collection. All analog signals were continuously digitalized with an appropriate system (Codas, DataQ, Akron, OH). The pulmonary pressure and flow waves were sampled at 200 Hz and stored. Cardiac cycles were defined by R-wave detection provided by a permanent recording of a one-lead electrocardiogram. Ten consecutive cycles were recorded during apnea and were numerically averaged to obtain representative diagrams of pressure and flow waves, corresponding to specific experimental conditions. Simultaneously, 10 consecutive RV PV loops were recorded. The same measurements were then repeated during transient occlusion of the inferior vena cava using the Fogarty balloon.

Data analysis. We used a lumped parameter model, i.e., the three-element windkessel model (WK3), to analyze the flow conditions in the pulmonary circulation throughout the experimental protocol (Fig. 1). The 10 steady-state beats were analyzed under each condition (baseline, each 30 min after pulmonary embolism in *group A* or endotoxin infusion in *group B*), and the results were averaged. Maximal and minimal pulmonary arterial pressure defined systolic and diastolic pressures, respectively. Systolic ejection interval (t_s) was measured from the foot of the pulmonary arterial pressure wave to its incisura, and the diastolic interval was $t_d = T - t_s$, where T is the cardiac length. Pairs of pressure and flow data for each beat were analyzed, and the three elements of the model were simultaneously calculated by using an original analytic procedure, as described previously (12).

RV PV loops were obtained using the conductance catheter method (3). Pes was the pressure at maximal ventricular elastance (E_{max}) for a steady-state loop. Maximal RV elastance was determined as $\{P(t)/[V(t) - V_o]\}_{max}$, where $P(t)$ and $V(t)$ are instantaneous RV pressure and volume, respectively; and V_o is the volume intercept of the end-systolic PV relation obtained using the preload reduction method (3).

E_a definitions. An expression of the effective E_a with the three parameters of the WK3 is given by (12, 21, 24):

$$E_a(WK) = RT/[t_s + \tau(1 - e^{-td/\tau})] \quad (1)$$

where RT is the total pulmonary vascular resistance, i.e., the sum of the characteristic resistance (R_1) and the pulmonary arteriolar resis-

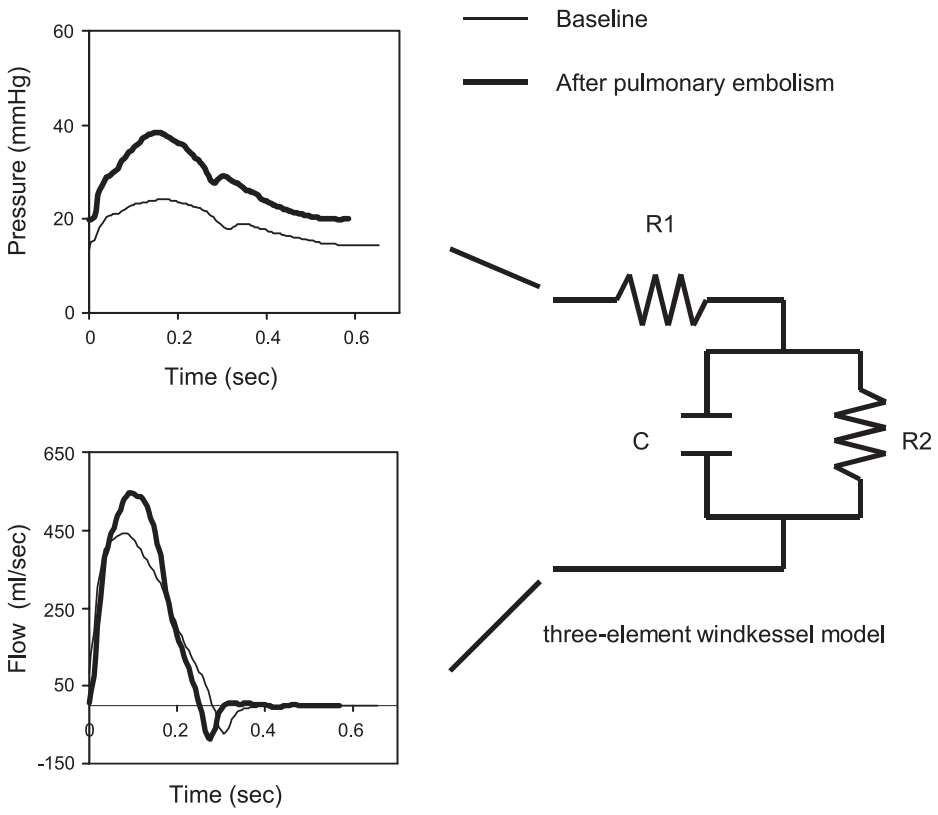

Fig. 1. Representation of the three-element windkessel model (WK) with an example of computer record used to obtain averaged pulmonary pressure (*top*) and flow (*bottom*) waveforms from 10 consecutive systoles in a typical *group A* pig. R_1, characteristic vascular resistance; C, vascular compliance; R_2, peripheral vascular resistance.

Table 1. *Effects of induced pulmonary hypertension on heart rate, cardiac output, systemic and pulmonary arterial pressures, and left and right atrial pressures*

	HR, beats/min	CO, l/min	MAP, mmHg	PAP_{mean}, mmHg	Pla, mmHg	Pra, mmHg
			Group A			
T0	104±4	5.1±0.2	82±9	11±3	7±1	7±2
PHT	114±4	4.8±0.2	76±12	23±3	6±2	20±4
P	NS	<0.05	NS	<0.001	NS	<0.001
			Group B			
T0	114±2	4.8±0.9	75±13	15±2	8±2	8±2
PHT	124±3	4.3±1	60±8	25±2	6±2	22±2
P	NS	NS	NS	<0.001	NS	<0.001

Values are means ± SE. T0, baseline conditions; PHT, pulmonary hypertension; HR, heart rate; CO, cardiac output; MAP, mean arterial pressure; PAP_{mean}, mean pulmonary arterial pressure; Pla, left atrial pressure; Pra, right atrial pressure; NS, not significant.

tance (R_2); and τ is the diastolic pressure decay time constant or the product of R_2 and the total capacitance (C), which represents the compliant properties of the pulmonary arterial tree. The electrical representation of the WK3 is displayed in Fig. 1. The three elements of the model are calculated using an analytic procedure (12, 14). Details of this analysis are provided in the APPENDIX.

Eq. 1 can be simplified as follows. If the τ is long compared with the t_d ($\tau \gg t_d$), then the denominator reduces to $t_s + t_d = T$, the cardiac cycle length.

Thus

$$E_a(WK) \approx RT/T \quad (2)$$

However,

$$RT = (PAP_{mean} - Pla)/CO \quad (3)$$

Therefore,

$$E_a(WK) \approx (PAP_{mean} - Pla)/(CO \cdot T) = (PAP_{mean} - Pla)/(SV \cdot HR \cdot T) = (PAP_{mean} - Pla)/SV \quad (4)$$

If PAP_{mean} is further approximated by RV Pes, then

$$E_a(WK) \approx (PAP_{mean} - Pla)/SV \approx (Pes - Pla)/SV = E_a * (PV) \quad (5)$$

If the downstream pressure can be neglected as in the systemic circulation, then

$$E_a(WK) \approx Pes/SV = E_a(PV) \quad (6)$$

Statistical analysis. For each group, we performed a linear regression between E_a(WK) and E_a(PV), and we completed the analysis with a Bland-Altman test (Statistica version 7, StatSoft). Changes in hemodynamics and WK3 parameters were evaluated by a repeated-measures analysis of variance (Statistica version 7, StatSoft). Data are expressed as means ± SE.

RESULTS

Windkessel parameters and PV loop effects of arterial load variations. The effects of induced pulmonary hypertension in both groups on HR, CO, mean arterial pressure, PAP_{mean}, Pla, and right atrial pressure are shown in Table 1. In *group A*, pulmonary embolism was responsible for several alterations in the shape of pressure and flow waves, including early pressure inflection, late systolic peak pressure, and sharper pulmonary arterial flow waveform (Fig. 1). The corresponding PV loops became oblong due to a rise in ejection pressure (Fig. 2, *left*). In *group B*, administration of endotoxin induced a bulging of PV loops (Fig. 2, *right*). These modifications were related to both reduced arterial compliance and enhanced wave reflections. Clot embolism and infusion of endotoxin lead to significant changes in the windkessel parameters, as shown in Fig. 3. In *group A* (Fig. 3, *left*), R_1 did not change significantly; however, there was a rapid rise in R_2 and a fall in C after pulmonary embolism. In *group B* (Fig. 3, *right*), both R_1 and R_2 significantly increased following endotoxin insult, whereas C progressively decreased after endotoxin insult.

E_a(PV) compared with E_a(WK). The time course of both E_a(PV) and E_a(WK) in each group is shown in Fig. 4. In *group A*, E_a(PV) and E_a(WK) increased rapidly after the first vena cava injection of embols. In *group B*, both parameters progressively increased after endotoxin infusion. In each group, the pulmonary E_a calculated with the complex method [E_a(WK)] and the simple method [E_a(PV)] displayed a parallel evolution.

Despite the varying vascular properties due to either pulmonary embolism or endotoxin infusion, the ratio of ventricular Pes to SV [Pes/SV = E_a(PV)] was remarkably similar to E_a(WK) derived from the windkessel parameters using *Eq. 1*. However, E_a(PV) was somewhat higher than E_a(WK). The offset between E_a(PV) and E_a(WK) was significantly reduced by using E_a * (PV) instead of E_a(PV) (Fig. 4). Indeed, incorporating Pla into E_a(PV), the mean difference between both methods decreased from 0.24 ± 0.07 to 0.11 ± 0.08 mmHg/ml (means ± SD) in *group A* and from 0.29 ± 0.11 to 0.08 ± 0.1 mmHg/ml (means ± SD) in *group B* (Fig. 5).

The linear relations were nearly identical in both groups and given by E_a * (PV) = 0.92 E_a(WK) + 0.1 [$r^2 = 0.96$, $n = 56$, SE of estimate (SEE) = 0.1, $P < 0.0001$] in *group A*, and E_a * (PV) = 0.88 E_a(WK) + 0.19 ($r^2 = 0.97$, $n = 56$, SEE = 0.21, $P < 0.0001$) in *group B* (Fig. 5). The limits of agreement indicated that the differences between both methods did not exceed 0.08 mmHg/ml in *group A* and 0.11 mmHg/ml in *group B* for 95% of the cases (Fig. 5).

E_a(PV) and RT/T. As for the relation between E_a(PV) and E_a(WK), there was a strong linear correlation between E_a(PV)

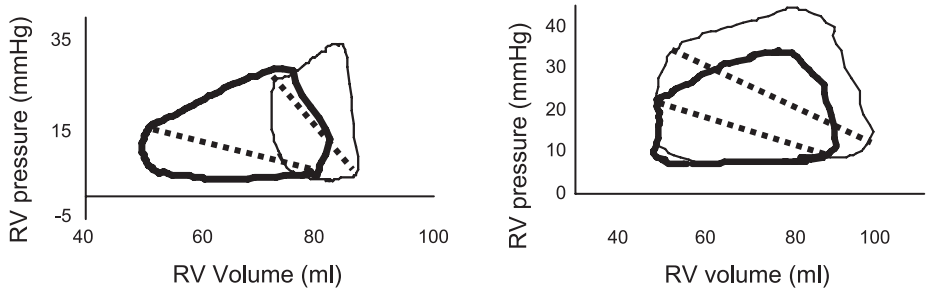

Fig. 2. Example of right ventricular (RV) pressure-volume (PV) loops in a *group A* pig (*left*) before (thick lines) and after (thin lines) pulmonary embolism, and in a *group B* pig (*right*) before (thick lines) and after (thin lines) endotoxin infusion. Lines representing E_a = (Pes − Pla)/SV, where E_a is arterial elastance, Pes is end-systolic pressure, Pla is left atrial pressure, and SV is stroke volume, are shown for each PV loop (dotted lines).

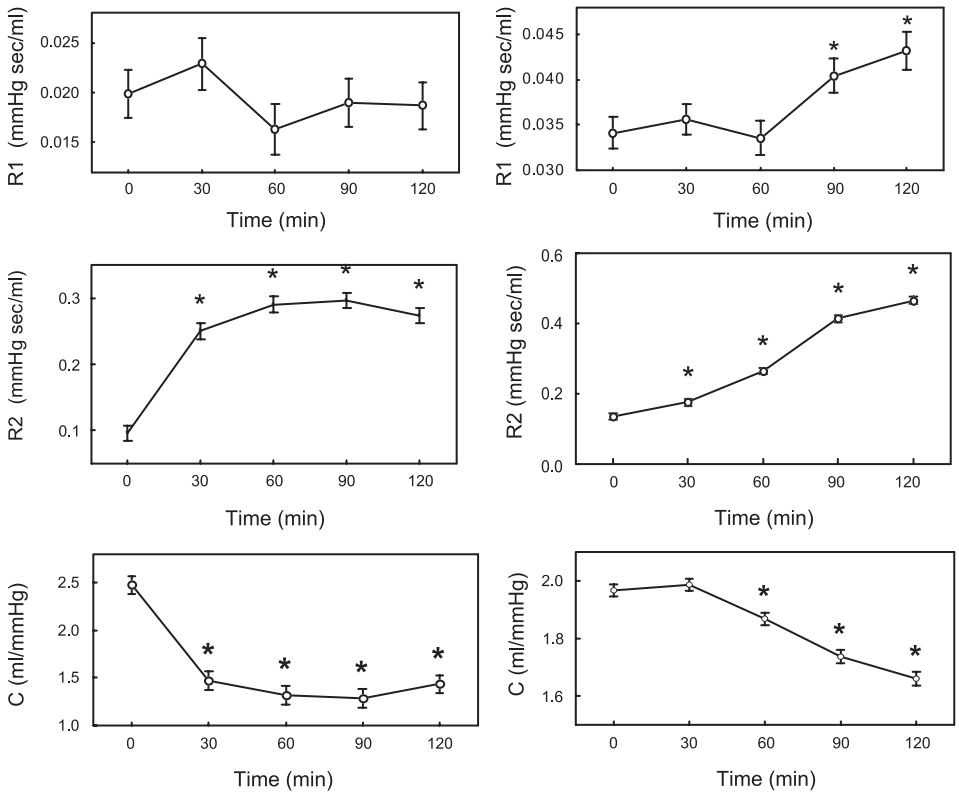

Fig. 3. Time course of WK parameters (R_1, R_2, C) in *groups A* (*left*) and *B* (*right*). *$P <$ 0.05 compared with baseline.

and RT/T: E_a(PV) = 1.1·RT/T + 0.27 (r^2 = 0.96, $P < 0.0001$, n = 58, SEE = 0.032) in *group A*, and E_a(PV) = 0.98·RT/T + 0.36 (r^2 = 0.97, $P < 0.0001$, n = 56, SEE = 0.059) in *group B*. The bias was still reduced using E_a ∗ (PV) instead of E_a(PV): E_a ∗ (PV) = 1.04·RT/T + 0.11 (r^2 = 0.93, $P <$ 0.0001, n = 58, SEE = 0.038) in *group A,* and E_a ∗ (PV) = 0.95·RT/T + 0.23 (r^2 = 0.96, $P < 0.0001$, n = 56, SEE = 0.051) in *group B*. The low SEE obtained in each group corresponded to a good agreement between both parameters (Fig. 6).

DISCUSSION

In the present study, we tested whether or not pulmonary vascular load could be assessed by the effective E_a determined by the simple ratio of Pes to SV [E_a(PV)]. Our results demonstrated that there was an excellent correlation between E_a(WK) calculated from the windkessel model and E_a calculated as Pes/SV over a wide range of loading conditions resulting from either pulmonary embolism or endotoxin insult. However, the effective E_a determined by the simple ratio of Pes to SV consistently exceeded the elastance calculated from the windkessel parameters. The offset between E_a(PV) and E_a(WK) nearly vanished using E_a ∗ (PV), which incorporates Pla, instead of E_a(PV). This observation implies that, contrary to what is observed in the systemic circulation, the effect of the downstream pressure on the pulmonary circulation is not negligible. Sagawa et al. suggested incorporating the presence of an effective downstream pressure into E_a (21). Nevertheless, Pla is frequently ignored in the pulmonary circulation, and E_a is calculated as the ratio of Pes to SV similarly to the systemic circulation (4, 9, 18, 28).

The linear relations between E_a ∗ (PV) and E_a(WK) were nearly identical in both groups. These results are concordant with those of Kelly et al. (10) in the systemic circulation, who

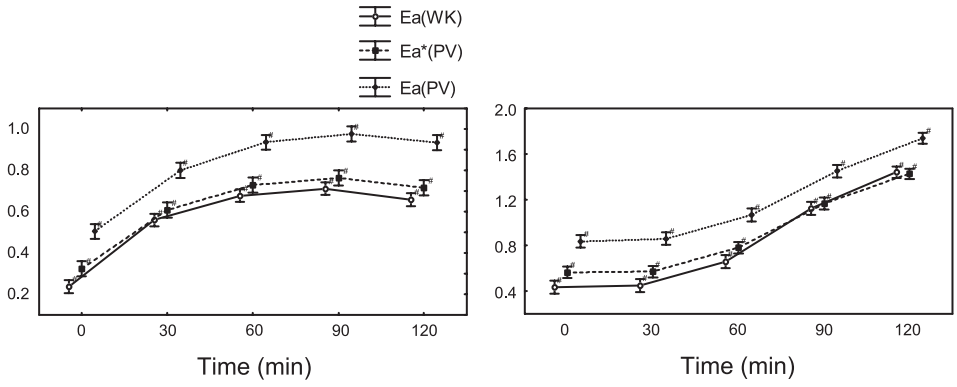

Fig. 4. Time course of E_a(WK), E_a ∗ (PV), and E_a(PV) in *groups A* (*left*) and *B* (*right*). #$P <$ 0.05 compared with baseline.

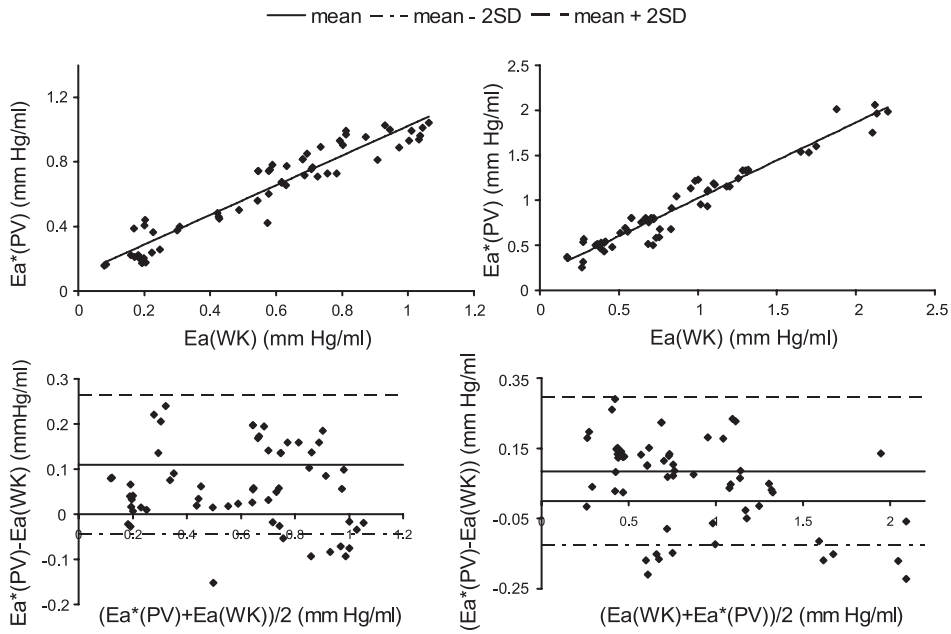

Fig. 5. *Top*: correlation between E_a * (PV) and E_a(WK): E_a * (PV) = 0.92 E_a(WK) + 0.1 [r^2 = 0.96, n = 56, SE of estimate (SEE) = 0.1, $P < 0.0001$] in *group A* (*left*), and E_a * (PV) = 0.88 E_a(WK) + 0.19 (r^2 = 0.97, n = 56, SEE = 0.21, $P < 0.0001$) in *group B* (*right*). *Bottom*: Bland-Altman test compares E_a * (PV) and E_a(WK) in *groups A* (*left*) and *B* (*right*). The solid line is the mean difference; the dashed lines represent mean difference ±2 SD.

showed that E_a(PV) provides a useful method to assess arterial load and its interaction with the human ventricle. These authors suggested that E_a(PV) is a powerful tool to assess the effects of increased pulsatile load caused by aging or hypertension on PV loops. They also pointed out that mean arterial resistance often underestimates the real effects of the load on cardiac performance (10). Segers et al. (23) found that E_a(PV) underestimated E_a(WK) provided by the four-element windkessel model.

Our results demonstrated that E_a * (PV) can be used in place of E_a(WK) in the pulmonary circulation. The correlation between E_a * (PV) and E_a(WK) was excellent in normal conditions, as well as after pulmonary embolism or endotoxin infusion, as shown by the Bland-Altman test in both groups. In *group A*, E_a showed an asymptotic increase early after the pulmonary embolism, in concordance with an acute loss of compliance and a rapid rise of the total resistance offered by the pulmonary vascular tree. In *group B*, E_a progressively increased with an exponential trend associated with a progressive decrease in compliance and a slow rise in the total resistance of the pulmonary vasculature. Although experimental conditions were totally different, the linear correlations between both methods in each group were nearly similar.

Our data showed that pulmonary embolism or endotoxin insult led to a complex pulmonary vascular response involving a dynamic, time-dependent interplay between R_1, C, and R_2. Nevertheless, the correlation between both methods in each group remained excellent over the range of important variations in the windkessel parameters.

The ratio of E_{max} on E_a (E_{max}/E_a) is superior to one in the normal heart, suggesting that the ventricle operates close to the optimal efficiency. Our laboratory previously showed that, in heart failure due to pulmonary embolism and sepsis, the decreased value of E_{max}/E_a was related to an impaired use of energy by the failing heart (6, 13, 15). In combination with E_{max}, E_a(PV) appears to be a simple way to characterize ventriculo-arterial interaction (18, 26, 27). For the systemic circulation, Segers et al. (23) suggested that E_a can be approximated by RT/T only for high C values. For the pulmonary circulation, our results evidenced significant correlation between both methods, as well as between E_a * (PV) and RT/T, despite dramatic changes in pulmonary vascular compliance. Our laboratory previously showed a concordant evolution between E_{max}/E_a and stroke work in pulmonary embolism or septic shock (6, 13, 15). This could be explained by higher basal pulmonary vascular compliance compared with the values obtained on the systemic circuit.

The determination of E_a as the simple ratio of Pes minus Pla to SV to assess pulmonary vascular load is rapidly and easily feasible in clinical settings. In contrast, E_a(WK) requires invasive measurement of pulmonary flow and pressure waves, which limits its potential use (8, 19).

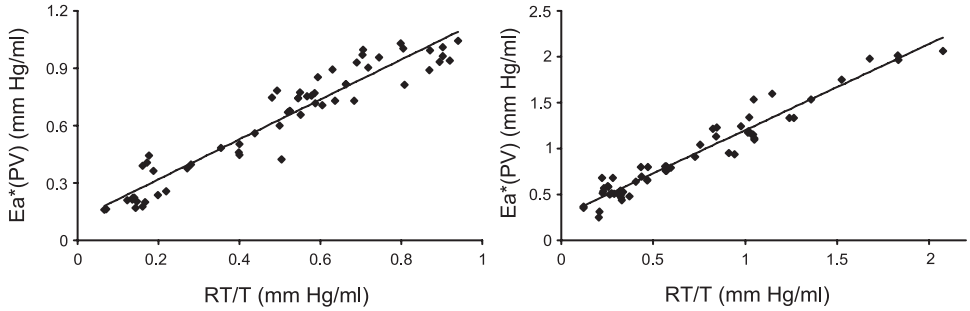

Fig. 6. Correlation between E_a * (PV) and total pulmonary vascular resistance (RT)/cardiac length (T) is given by the following linear relations: E_a * (PV) = 1.04·RT/T + 0.11 (r^2 = 0.93, $P < 0.0001$, n = 58, SEE = 0.038) (*group A*; *left*), and E_a * (PV) = 0.95·RT/T + 0.23 (r^2 = 0.96, $P < 0.0001$, n = 56, SEE = 0.051) (*group B*; *right*).

RV tolerance and adaptation to chronic or acute increase in pulmonary vascular load may be a cornerstone in the prognosis of patients suffering from pulmonary hypertension. Therefore, evaluation of RV-pulmonary arterial coupling by using the ratio of contractility, assessed by the slope of the end-systolic PV relationship, to E_a seems essential to evaluate correctly the facilitation of energy transfer from the RV into the pulmonary circuit (11). However, determination of E_{max} requires preload variation that is difficult to apply in clinical practice. It is the reason why single-beat methods have been developed, but unfortunately not yet validated for the RV. Therefore, further studies should be encouraged (16, 22). As pathophysiological RV conditions are often associated with valve insufficiencies, SV was derived from pulmonary arterial flow divided by HR.

Some study limitations should be acknowledged. E_a(WK) and E_a * (PV) were related through two assumptions (*Eqs. 2–6*). Diastolic time constant ($\tau = R_2 \cdot C$) is long relative to the diastolic time period (t_d), and Pes is approximately equal to PAP_{mean}. Compared with the systemic vasculature, lower pulmonary vasculature resistance is counterbalanced by higher pulmonary vascular compliance in such a way that the first assumption can be considered as valid in basal conditions. In pulmonary hypertension, rise in R_2 prevails on loss in C, so the first assumption holds. Because of lower pulmonary arterial pressure levels, discrepancy between Pes and PAP_{mean} is more important than in the systemic vascular tree. However, in pulmonary hypertension, due to higher pulmonary arterial pressure levels and enhanced wave reflections occurring during systole, PAP_{mean} tends to be nearer to Pes.

In summary, several recent studies highlighted the importance of abnormal pulsatile load effect in the mechanism of right heart failure (1, 2, 7, 20). Several methods to assess pulmonary vascular load have been proposed, but require a complete acquisition of pulmonary arterial pressure and flow waveforms. As a result, such methods are difficult to apply in current clinical practice. In the present study, we suggest that pulmonary arterial load can be simply assessed from the ratio of RV Pes minus Pla to RV SV in the setting of pulmonary hypertension. The downstream pressure plays an important role in the pulmonary circulation and should be incorporated into the pulmonary effective E_a.

APPENDIX: CALCULATION OF WK3 PARAMETERS

The relationship between pressure and flow in the electrical representation of WK3 is described by the following equation:

$$P(t) + R_2C\frac{dP(t)}{dt} = (R_1 + R_2)\dot{Q}(t) + R_1R_2C\frac{d\dot{Q}(t)}{dt} \qquad (A1)$$

where $\dot{Q}$ is pulmonary flow; P is pulmonary arterial pressure; and t_0 is the beginning of the cardiac cycle, defined as the R wave on the ECG. R_1, R_2, and C are the three elements of the WK3 (Fig. 1). *Eq. A1* is integrated and becomes:

$$\int_{t_0}^{t} Q(\tau)d\tau = k_1\int_{t_0}^{t} P(\tau)d\tau + k_2(P(t) - P(t_0)) + k_3(\dot{Q}(t) - Q(t_0)) \qquad (A2)$$

where

$$k_1 = \frac{1}{R_1 + R_2}, \quad k_2 = \frac{CR_2}{R_1 + R_2}, \quad \text{and} \quad k_3 = -\frac{CR_2}{R_1 + R_2} \qquad (A3)$$

The multiple-regression technique estimates the constants k_i to minimize the residual sum of squares (RSS), i.e., the sum of squared differences between the observed values of both parts of this equation

$$RSS = \sum_t \left[\int_{t_0}^{t} \dot{Q}(\tau)d(\tau) - k_1\int_{t_0}^{t} P(\tau)d\tau - k_2[P(t) - P(t_0)] - k_3[\dot{Q}(t) - \dot{Q}(t_0)]\right]^2 \qquad (A4)$$

R_1, R_2, and C values are then derived by solving *Eq. A3*.

GRANTS

This work was supported by a grant from the Leon Fredericq Foundation of the University of Liege (Belgium).

REFERENCES

1. **Castelain V, Herve P, Lecarpentier Y, Duroux P, Simonneau G, Chemla D.** Pulmonary artery pulse pressure and wave reflection in chronic pulmonary thromboembolism and primary pulmonary hypertension. *J Am Coll Cardiol* 37: 1085–1092, 2001.
2. **Chemla D, Castelain V, Simonneau G, Lecarpentier Y, Herve P.** Pulse wave reflection in pulmonary hypertension. *J Am Coll Cardiol* 39: 743–744, 2002.
3. **Dickstein ML, Yano O, Spotnitz HM, Burkhoff D.** Assessment of right ventricular contractile state with the conductance catheter technique in the pig. *Cardiovasc Res* 29: 820–826, 1995.
4. **Fourie PR, Coetzee AR, Bolliger CT.** Pulmonary artery compliance: its role in right ventricular-arterial coupling. *Cardiovasc Res* 26: 839–844, 1992.
5. **Furuno Y, Nagamoto Y, Fujita M, Kaku T, Sakurai S, Kuroiwa A.** Reflection as a cause of mid-systolic deceleration of pulmonary flow wave in dogs with acute pulmonary hypertension: comparison of pulmonary artery constriction with pulmonary embolisation. *Cardiovasc Res* 25: 118–124, 1991.
6. **Ghuysen A, Lambermont B, Dogne JM, Kolh P, Tchana-Sato V, Morimont P, Magis D, Hanson J, Segers P, D'Orio V.** Effect of BM-573 {*N*-terbutyl-*N*′-[2-(4′-methylphenylamino)-5-nitro-benzenesulfonyl]urea}, a dual thromboxane synthase inhibitor and thromboxane receptor antagonist, in a porcine model of acute pulmonary embolism. *J Pharmacol Exp Ther* 310: 964–972, 2004.
7. **Grant BJ, Lieber BB.** Clinical significance of pulmonary arterial input impedance. *Eur Respir J* 9: 2196–2199, 1996.
8. **Huez S, Brimioulle S, Naeije R, Vachiery JL.** Feasibility of routine pulmonary arterial impedance measurements in pulmonary hypertension. *Chest* 125: 2121–2128, 2004.
9. **Kass A, Kelly RP.** Ventriculo-arterial coupling: concepts, assumptions, and applications. *Ann Biomed Eng* 20: 41–62, 1992.
10. **Kelly RP, Ting CT, Yang TM, Liu CP, Maughan WL, Chang MS, Kass DA.** Effective arterial elastance as index of arterial vascular load in humans. *Circulation* 86: 513–521, 1992.
11. **Lambermont B, D'Orio V.** The role of right ventricular-pulmonary arterial coupling to differentiate between effects of inotropic agents in experimental right heart failure. *Crit Care Med* 34: 2864–2865, 2006.
12. **Lambermont B, D'Orio V, Gerard P, Kolh P, Detry O, Marcelle R.** Time domain method to identify simultaneously parameters of the wind-kessel model applied to the pulmonary circulation. *Arch Physiol Biochem* 106: 245–252, 1998.
13. **Lambermont B, Ghuysen A, Kolh P, Tchana-Sato V, Segers P, Gerard P, Morimont P, Magis D, Dogne JM, Masereel B, D'Orio V.** Effects of endotoxic shock on right ventricular systolic function and mechanical efficiency. *Cardiovasc Res* 59: 412–418, 2003.
14. **Lambermont B, Kolh P, Detry O, Gerard P, Marcelle R, D'Orio V.** Analysis of endotoxin effects on the intact pulmonary circulation. *Cardiovasc Res* 41: 275–281, 1999.
15. **Lambermont B, Kolh P, Dogne JM, Ghuysen A, Tchana-Sato V, Morimont P, Benoit P, Gerard P, Masereel B, Limet R, D'Orio V.** Effects of U-46619 on pulmonary hemodynamics before and after administration of BM-573, a novel thromboxane A2 inhibitor. *Arch Physiol Biochem* 111: 217–223, 2003.
16. **Lambermont B, Segers P, Ghuysen A, Tchana-Sato V, Morimont P, Dogne JM, Kolh P, Gerard P, D'Orio V.** Comparison between single-

beat and multiple-beat methods for estimation of right ventricular contractility. *Crit Care Med* 32: 1886–1890, 2004.
17. **Lankhaar JW, Westerhof N, Faes TJ, Marques KM, Marcus JT, Postmus PE, Vonk-Noordegraaf A.** Quantification of right ventricular afterload in patients with and without pulmonary hypertension. *Am J Physiol Heart Circ Physiol* 291: H1731–H1737, 2006.
18. **Missant C, Rex S, Segers P, Wouters PF.** Levosimendan improves right ventriculovascular coupling in a porcine model of right ventricular dysfunction. *Crit Care Med* 35: 707–715, 2007.
19. **Muthurangu V, Atkinson D, Sermesant M, Miquel ME, Hegde S, Johnson R, Andriantsimiavona R, Taylor AM, Baker E, Tulloh R, Hill D, Razavi RS.** Measurement of total pulmonary arterial compliance using invasive pressure monitoring and MR flow quantification during MR-guided cardiac catheterization. *Am J Physiol Heart Circ Physiol* 289: H1301–H1306, 2005.
20. **Naeije R.** Pulmonary vascular resistance. A meaningless variable? *Intensive Care Med* 29: 526–529, 2003.
21. **Sagawa K, Maughan L, Hiroyugi S, Sunagawa K.** *Cardiac Contraction and the Pressure-Volume Relationship.* New York: Oxford University Press, 1988, p. 238–240.
22. **Schenk S, Popovic ZB, Ochiai Y, Casas F, McCarthy PM, Starling RC, Kopcak MW Jr, Dessoffy R, Navia JL, Greenberg NL, Thomas JD, Fukamachi K.** Preload-adjusted right ventricular maximal power: concept and validation. *Am J Physiol Heart Circ Physiol* 287: H1632–H1640, 2004.
23. **Segers P, Stergiopulos N, Westerhof N.** Relation of effective arterial elastance to arterial system properties. *Am J Physiol Heart Circ Physiol* 282: H1041–H1046, 2002.
24. **Sunagawa K, Maughan WL, Burkhoff D, Sagawa K.** Left ventricular interaction with arterial load studied in isolated canine ventricle. *Am J Physiol Heart Circ Physiol* 245: H773–H780, 1983.
25. **Sunagawa K, Maughan WL, Sagawa K.** Optimal arterial resistance for the maximal stroke work studied in isolated canine left ventricle. *Circ Res* 56: 586–595, 1985.
26. **Sunagawa K, Sugimachi M, Todaka K, Kobota T, Hayashida K, Itaya R, Chishaki A, Takeshita A.** Optimal coupling of the left ventricle with the arterial system. *Basic Res Cardiol* 88, *Suppl* 2: 75–90, 1993.
27. **Takaoka H, Takeuchi M, Odake M, Hayashi Y, Mori M, Hata K, Yokoyama M.** Comparison of the effects on arterial-ventricular coupling between phosphodiesterase inhibitor and dobutamine in the diseases human heart. *J Am Coll Cardiol* 22: 598–606, 1993.
28. **Wauthy P, Pagnamenta A, Vassalli F, Naeije R, Brimioulle S.** Right ventricular adaptation to pulmonary hypertension: an interspecies comparison. *Am J Physiol Heart Circ Physiol* 286: H1441–H1447, 2004.